

# Preparation and Adsorption Properties of Magnetic $\text{Co}_{0.5}\text{Ni}_{0.5}\text{Fe}_2\text{O}_4$ –Chitosan Nanoparticles<sup>1</sup>

D. Jia<sup>a</sup>, D. Wang<sup>b</sup>, H. Wu<sup>c</sup>, and Q. Lian<sup>a</sup>

<sup>a</sup> College of Chemical Engineering,  
Hebei Normal University of Science and Technology, Qinhuangdao, 066600 China

<sup>b</sup> Analysis and Testing Center,  
Hebei Normal University of Science and Technology, Qinhuangdao, 066600 China

<sup>c</sup> Chemical and Pharmaceutical Engineering,  
Hebei University of Science and Technology, Shijiazhuang, 050018 China  
e-mail: lianqilianqi517@163.com

Received February 8, 2015

**Abstract**—Magnetic chitosan microspheres were prepared by the emulsification cross-linking technique in the presence of glutaraldehyde as cross-linking agent, liquid paraffin as dispersant, and Span-80 as emulsifier. The optimal cross-linking time and  $\text{Co}_{0.5}\text{Ni}_{0.5}\text{Fe}_2\text{O}_4$  : chitosan ratio were determined. The morphology of particles was studied by different techniques. The adsorption characteristics were studied and the effect exerted by the initial concentration of methyl orange, the time of cross-linking, and the amount of the adsorbent was determined. It is found that the product obtained at the  $\text{Co}_{0.5}\text{Ni}_{0.5}\text{Fe}_2\text{O}_4$  : chitosan ratio 1 : 4 and the cross-linking time 5 h has the uniform morphology. At room temperature, the  $\text{Co}_{0.5}\text{Ni}_{0.5}\text{Fe}_2\text{O}_4$ –chitosan magnetic composite has maximal adsorption for methyl orange at the dosage 20 mg.

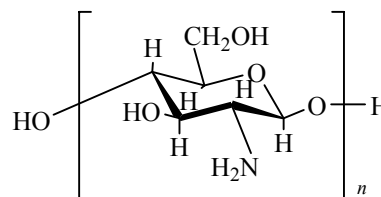
**Keywords:** magnetic, chitosan, emulsification cross-linking, adsorption

**DOI:** 10.1134/S1070363216030294

## INTRODUCTION

The past few years have witnessed rapidly expanding interest in renewable raw materials and marine food waste as sources of biomolecules with potential to replace synthetic polymers in fabricating biocompatible, bioactive, and biodegradable materials for unique applications [1, 2]. Since biomolecules became more available, there is ever-increasing demand for high-performance “natural” matrices for biomedical and pharmaceutical applications such as organ regeneration and tissue engineering [3], wound dressing [4], medical suture line, artificial limb, controlled drug delivery systems [5, 6], films, contact lenses, and capsules for oral ingestion [3], which has stimulated development of smart matrices able to sense environmental changes (pH, temperature, and ionic strength) and trigger release of active and bioactive compounds.

The chemical formula of chitosan is:



Chitosan magnetic composites are a new type of functional polymers, which are core-shell structures consisting of a chitosan cross-linked magnetic core and chitosan shell. Surface magnetic chitosan microspheres contain hydroxyl, amino, and other groups and exhibit excellent adsorption properties for acid and reactive dyes. At the same time, a number of these groups can form stable chelated metal ions suitable for effective adsorption and trapping of heavy metal ions from a solution [8].

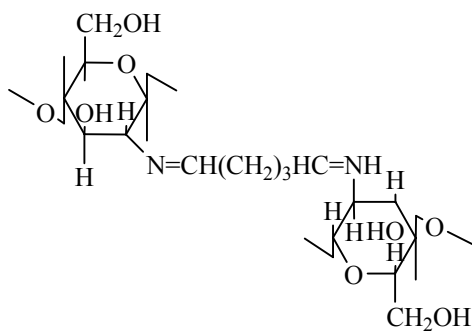
The schematic cross-linking diagram is in Scheme 1.

The protonation is described by the Scheme 2.

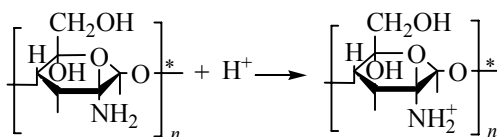
Magnetic chitosan is better adsorbent for  $\text{Hg}^{2+}$ ,  $\text{Cr}^{3+}$ ,  $\text{Ni}^{2+}$ , and other heavy metal ions. In addition, the surface amino group of magnetic chitosan

<sup>1</sup> The text was submitted by the authors in English.

Scheme 1.



Scheme 2.



microspheres can react with carboxyl groups of the protein molecules to cause their adsorption on the surface, which makes magnetic chitosan a suitable carrier for enzyme immobilization. The advantage of magnetic chitosan as carrier is safety and biocompatibility. Therefore, the study of the magnetic chitosan composites is urgent.

## EXPERIMENTAL

**Reagents.** Chitosan (95.5% diacetylated,  $M_w = 1.0 \times 10^5$ ) was purchased from the YuHuan Chemical Company (China). A glutaraldehyde solution (50%), Span-80, liquid paraffin, petroleum ether, ethanol, glacial acetic acid, sodium hydroxide (NaOH), acetone, and  $\text{Co}_{0.5}\text{Ni}_{0.5}\text{Fe}_2\text{O}_4$  were home-made reagents.

**Preparation of magnetic chitosan nanoparticles.** 0.5 g of  $\text{Co}_{0.5}\text{Ni}_{0.5}\text{Fe}_2\text{O}_4$  magnetic particles was quickly introduced into a 5% acetic acid (40 mL) containing 2 g of chitosan (i.e., the  $\text{Co}_{0.5}\text{Ni}_{0.5}\text{Fe}_2\text{O}_4$  to chitosan ratio was 1 : 4). The solution was transferred into an ultrasonic reactor and ground there for 10 min to ensure the uniform size for chitosan and magnetic particles. The ultrasonic frequency was 22 kHz and the power, 1000 W. After that, 40 mL of liquid paraffin and 10 drops of Span-80 were added. Then, the solution was placed in an ultrasonic reactor for 30 min (frequency 22 kHz, power 500 W). To get better magnetic properties, the reaction systems were kept in a water bath at 60°C for 5 h. To form cross-linked magnetic chitosan nanoparticles, 2 mL of glutaral-

dehyde was added and the system was kept for 5 h under the same conditions. After the reaction was complete, the prepared nanoparticles were precipitated by centrifugation at a speed of 8000 rpm for 1 h, rinsed with ethanol and deionized water for four times, and freeze-dried for 24 h.

**Characterization of magnetic chitosan nanoparticles.** *X-ray diffraction (XRD).* X-ray powder diffraction (XRD) patterns were measured with a Bruker D8 diffractometer in a monochromatized  $\text{CuK}\alpha$ -radiation ( $\lambda = 1.5426 \text{ \AA}$ , voltage 40 kV, current 30 mA).

*Fourier transform infrared (FTIR) spectroscopy.* FTIR spectra of the particles were recorded on a Prestige-21 spectrophotometer (Shimadzu).

*Transmission electron microscopy (TEM).* The size and morphology of  $\text{Co}_{0.5}\text{Ni}_{0.5}\text{Fe}_2\text{O}_4$ -chitosan magnetic nanoparticles were determined with an H-7650 TEM microscope (Hitachi). To do this, a drop of ethyl alcohol nanoparticle dispersion was poured onto a copper microgrid and evaporated at 20°C.

*Scanning electron microscopy (SEM).* The images of the surface of magnetic particles were obtained with a Kyky-2800 scanning electron microscope (Madell). Elemental analysis of the particles was done on a Vario EL III elemental analyzer (Elementar). The magnetic properties were determined with a PPMS-9 vibrating sample magnetometer (Quantum Design). The mass of a test powder was measured with high accuracy in a Teflon-coated sample holder.

*Adsorption.* Magnetic chitosan nanoparticles were introduced into a methyl orange solution of a prescribed concentration. Samples (5 mL) were taken above the solution at regular intervals and their absorbance was measured. The adsorption was determined from the change in the absorbance of a methyl orange solution by the following formula:

$$D = \frac{A_e - A_0}{A_0} \times 100\%, \quad (1)$$

where  $D$  is decoloration and  $A_0$  and  $A_e$  are the absorbances of the solution before and after the adsorption.

## RESULTS AND DISCUSSION

**Results of FTIR analysis.** FTIR spectra of the  $\text{Co}_{0.5}\text{Ni}_{0.5}\text{Fe}_2\text{O}_4$  particles, chitosan particles, and  $\text{Co}_{0.5}\text{Ni}_{0.5}\text{Fe}_2\text{O}_4$ -chitosan nanoparticles are demonstrated in Fig. 1 (curves 1–3), respectively. As seen, the

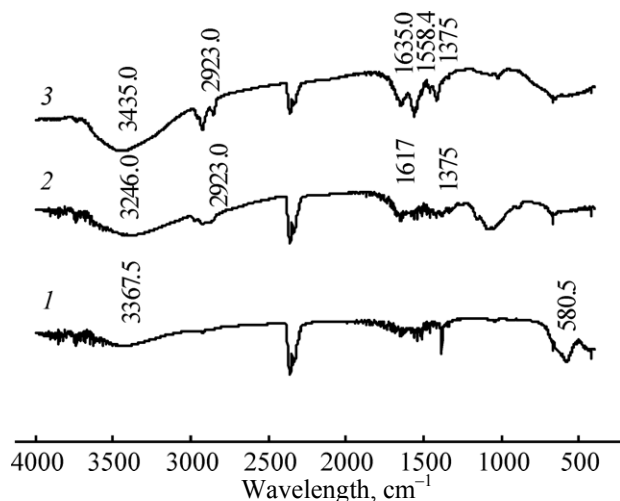


**Fig. 1.** FTIR spectra of (1) magnetic  $\text{Co}_{0.5}\text{Ni}_{0.5}\text{Fe}_2\text{O}_4$  particles, (2) chitosan particles, and (3) magnetic chitosan particles.

spectrum c has a new absorption peak of the Schiff base at  $1635\text{ cm}^{-1}$ , indicating that glutaraldehyde is indeed involved in the cross-linking reaction. The peak at  $580.5\text{ cm}^{-1}$  is a characteristic of the magnetic  $\text{Co}_{0.5}\text{Ni}_{0.5}\text{Fe}_2\text{O}_4$  particles, which shows that they are effectively cross-linked with chitosan particles. The spectrum 2 has peaks between  $\sim 3200\text{--}3400\text{ cm}^{-1}$ , which are due to the stretching vibrations of the  $\text{--OH}$  group in chitosan and due to hydrogen bonding, peaks between  $\sim 3400\text{--}3500\text{ cm}^{-1}$  attributable to stretching vibrations of the  $\text{N--H}$  bond, peak around  $2900\text{ cm}^{-1}$  assignable to  $\text{C--H}$  stretching vibrations, peak at  $1617\text{ cm}^{-1}$  attributable to the amide bond in chitosan, and peak of the  $\text{--CH}_3$  and  $\text{--CH}_2$  groups at  $1375\text{ cm}^{-1}$ . The spectrum of the composite contains all peaks

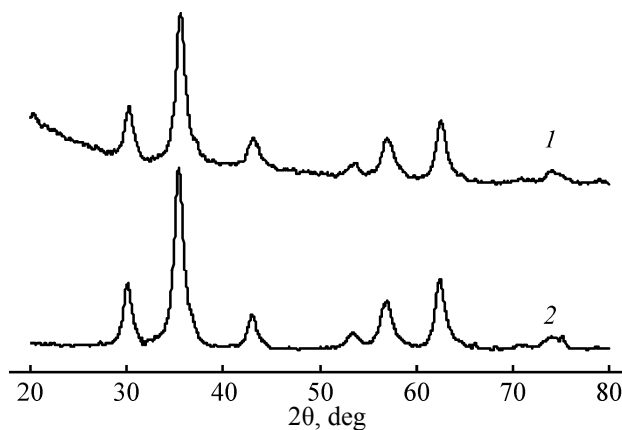


**Fig. 2.** X-ray diffraction patterns of (1) magnetic chitosan and (2) magnetic  $\text{Co}_{0.5}\text{Ni}_{0.5}\text{Fe}_2\text{O}_4$  particles.

present in the spectra 1 and 2, indicative of successful encapsulation of  $\text{Co}_{0.5}\text{Ni}_{0.5}\text{Fe}_2\text{O}_4$  magnetic particles with chitosan particles.

**Data on XRD.** In the diffraction patterns, reflections due to magnetic chitosan particles and bare  $\text{Co}_{0.5}\text{Ni}_{0.5}\text{Fe}_2\text{O}_4$  particles mostly coincide, which shows that the magnetic chitosan particles are a combination of chitosan and  $\text{Co}_{0.5}\text{Ni}_{0.5}\text{Fe}_2\text{O}_4$  (Fig. 2).

**Results of TEM.** The TEM images of the  $\text{Co}_{0.5}\text{Ni}_{0.5}\text{Fe}_2\text{O}_4$  particles and  $\text{Co}_{0.5}\text{Ni}_{0.5}\text{Fe}_2\text{O}_4$ -chitosan nanoparticles are demonstrated in Figs. 3a, 3b. As seen, the composite microspheres have the core-shell structure, with most  $\text{Co}_{0.5}\text{Ni}_{0.5}\text{Fe}_2\text{O}_4$  particles encapsulated into the chitosan shell.

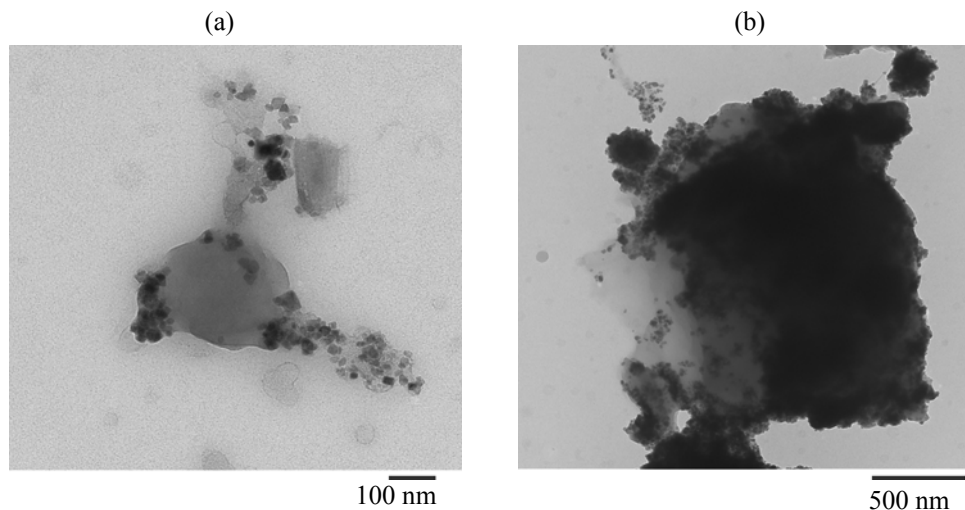


**Fig. 3.** The TEM micrograph of the magnetic (a)  $\text{Co}_{0.5}\text{Ni}_{0.5}\text{Fe}_2\text{O}_4$  particles and (b)  $\text{Co}_{0.5}\text{Ni}_{0.5}\text{Fe}_2\text{O}_4$ -chitosan composite microspheres.

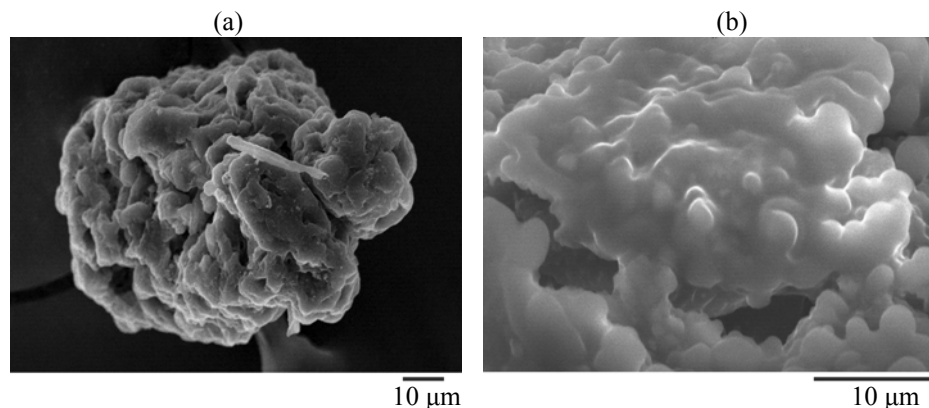


**Fig. 4.** The SEM micrograph of the magnetic (a)  $\text{Co}_{0.5}\text{Ni}_{0.5}\text{Fe}_2\text{O}_4$  particles and (b)  $\text{Co}_{0.5}\text{Ni}_{0.5}\text{Fe}_2\text{O}_4$ -chitosan composite microspheres.

**Results of SEM.** The SEM image of the magnetic  $\text{Co}_{0.5}\text{Ni}_{0.5}\text{Fe}_2\text{O}_4$ -chitosan particles at different magnifications is demonstrated in Figs. 4a, 4b. As seen, the surface of the magnetic chitosan particles is tightly wrapped and no particles of  $\text{Co}_{0.5}\text{Ni}_{0.5}\text{Fe}_2\text{O}_4$  are present. The  $\text{Co}_{0.5}\text{Ni}_{0.5}\text{Fe}_2\text{O}_4$  particles are successfully encapsulated into chitosan in a well shaped spherical form with a size of about  $150\ \mu\text{m}$ . This large sized is due to the large size of the  $\text{Co}_{0.5}\text{Ni}_{0.5}\text{Fe}_2\text{O}_4$  core (Fig. 4a). As seen from Fig. 4b, the chitosan coating is discontinuous and nonuniform.

**Data on the elemental analysis.** The elemental analysis of magnetic composite nanoparticles revealed Co, Ni, and Fe in the atomic ratio 4 : 1 : 1. This indicates that the  $\text{Co}_{0.5}\text{Ni}_{0.5}\text{Fe}_2\text{O}_4$  magnetic particles are encapsulated by chitosan particles integrally.

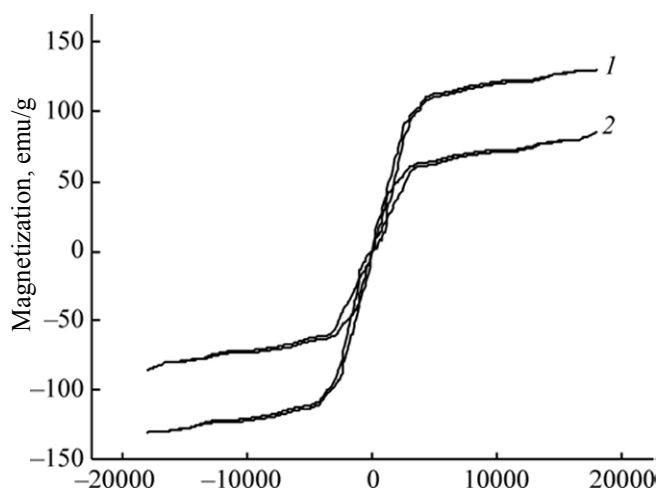


**Fig. 5.** Field dependence of the magnetization for (1)  $\text{Co}_{0.5}\text{Ni}_{0.5}\text{Fe}_2\text{O}_4$  nanoparticles and (2)  $\text{Co}_{0.5}\text{Ni}_{0.5}\text{Fe}_2\text{O}_4$ -chitosan nanoparticles.

**Results of a magnetization test.** One of distinct properties of magnetic nanoparticles is superparamagnetism, which arises if the magnetic anisotropy energy becomes comparable to thermal energy. The superparamagnetism is observed for particles less than 30 nm in diameter [9].

The magnetization curves of bare  $\text{Co}_{0.5}\text{Ni}_{0.5}\text{Fe}_2\text{O}_4$  particles and magnetic  $\text{Co}_{0.5}\text{Ni}_{0.5}\text{Fe}_2\text{O}_4$ -chitosan nanoparticles are shown in Fig. 5. As seen, the magnetization of bare  $\text{Co}_{0.5}\text{Ni}_{0.5}\text{Fe}_2\text{O}_4$  is higher than that of the magnetic  $\text{Co}_{0.5}\text{Ni}_{0.5}\text{Fe}_2\text{O}_4$ -chitosan nanoparticles (131.2 and 82.1 emu/g, respectively). Both particles reveal superparamagnetic properties.

**Adsorption of methyl orange from a solution.** The UV absorption spectrum of a methyl orange

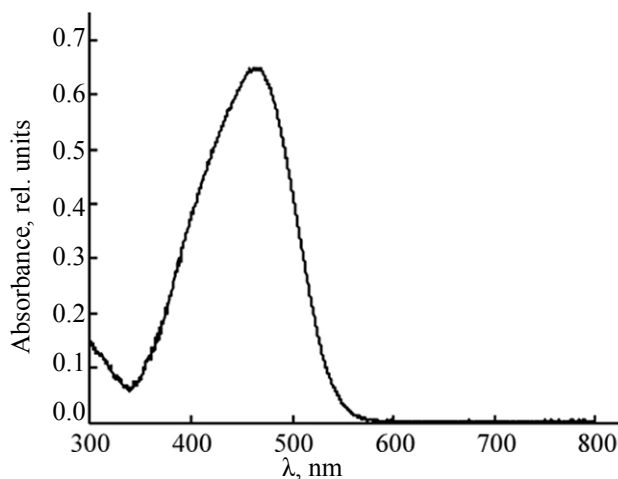


**Fig. 6.** UV absorption spectrum of a methyl orange solution.

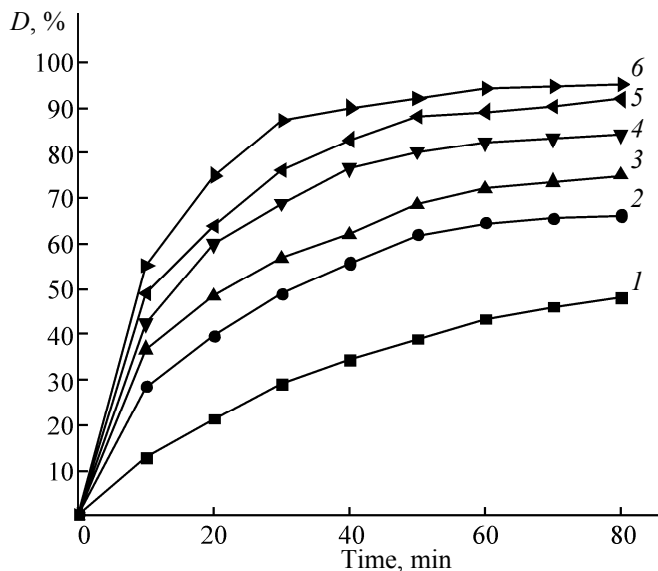


Fig. 7. The kinetic curves of decoloration at different amounts of the magnetic chitosan nanoparticles, mg: (1) 5, (2) 10, (3) 15, (4) 25, (5) 30, and (6) 20.

solution is demonstrated in Fig. 6. As seen, the methyl orange absorption has maximum at the wavelength 462 nm ( $\lambda_{\max} = 462$  nm).

Kinetic curves of decoloration of a methyl orange solution in the presence of magnetic  $\text{Co}_{0.5}\text{Ni}_{0.5}\text{Fe}_2\text{O}_4$ -chitosan nanoparticles are shown in Fig. 7. As seen, the adsorption amount and rate increase with increasing time. The decoloration effect also increases for larger doses of magnetic chitosan, reaching a maximal value at the dose 20 mg/L, after which it changes only slightly.

Experimental results showed that magnetic  $\text{Co}_{0.5}\text{Ni}_{0.5}\text{Fe}_2\text{O}_4$ -chitosan nanoparticles are good adsorbents for methyl orange, and consequently may be used for water treatment to remove dyes. Also they

may be used to sorb  $\text{Ca}^{2+}$ ,  $\text{Cd}^{2+}$ ,  $\text{Mo}^{6+}$ ,  $\text{Bi}^{3+}$ , and  $\text{Cu}^{2+}$  ions from industrial wastewater.

## CONCLUSIONS

In summary, novel  $\text{Co}_{0.5}\text{Ni}_{0.5}\text{Fe}_2\text{O}_4$ -chitosan nanoparticles with excellent core/shell structure and magnetic response properties were prepared. The superparamagnetic  $\text{Co}_{0.5}\text{Ni}_{0.5}\text{Fe}_2\text{O}_4$ -chitosan nanoparticles have good adsorption for methyl orange at the dosage 20 mg.

## ACKNOWLEDGMENTS

The study was supported by the Hebei Education Department (project no. Q2012056) and Qinhuangdao Science and Technology Bureau (project no. 2012021A127).

## REFERENCES

1. Tharanthan, R.N., *Trends Food Sci. Tech.*, 2003, vol. 14, p. 71.
2. Lin, C.C. and Metters, A.T., *Adv. Drug Deliver. Rev.*, 2006, vol. 58, p. 1379.
3. Khademhosseini, A. and Langer, R., *Biomater.*, 2007, vol. 28, p. 5087.
4. Ong, S.Y., Wu, J., Mochhala, S.M., Tan, M.H., and Lu, J., *Biomater.*, 2008, vol. 29, p. 4323.
5. Ghaffari, A., Navaee, K., Oshoui, M., Bayati, K., and Rafiee-Tehrani, M., *Eur. J. Pharm. Biopharm.*, 2007, vol. 67, p. 175.
6. Wei, X., Sun, N., Wu, B., Yin, C., and Wu, W., *Int. J. Pharmacol.*, 2006, vol. 318, p. 132.
7. Hoffiman, A.S., Stayton, P.S., Press, O., Murthy, N., Lackey, C.A., and Cheung, C., *Polym. Advan. Technol.*, 2002, vol. 13, p. 992.
8. Paulino, A.T., Santos, L.B., and Nozaki, J., *React. Funct. Polym.*, 2008, vol. 68, no. 2, pp. 634.
9. Josephson, L., US Patent 4672040.